Plasma Etoposide Catechol Increases in Pediatric Patients Undergoing Multiple-Day Chemotherapy with Etoposide

Naiyu Zheng,[1] Carolyn A. Felix,[2,3] Shaokun Pang,[1] Ray Boston,[4] Peter Moate,[4] Jennifer Scavuzzo,[2] and Ian A. Blair[1]

[1]Center for Cancer Pharmacology, Department of Pharmacology, University of Pennsylvania, Philadelphia; [2]Division of Oncology, The Children's Hospital of Philadelphia, Philadelphia; [3]Department of Pediatrics, University of Pennsylvania School of Medicine, Philadelphia; and [4]Biomathematics Unit, School of Veterinary Medicine, University of Pennsylvania, Kennett Square, Pennsylvania

ABSTRACT

Purpose: **The purpose of this research was to determine inter- and intrapatient differences in the pharmacokinetic profiles of etoposide and its genotoxic catechol metabolite during conventional multiple-day dosing of etoposide in pediatric patients.**

Experimental Design: **Seven pediatric patients with various malignancies received etoposide at a dose of 100 mg/m^2 i.v. over 1 h daily for 5 days. Blood samples were taken at selected time points on days 1 and 5. Plasma and protein-free plasma concentrations of etoposide and etoposide catechol were determined using a validated liquid chromatography/tandem mass spectrometry assay. Pharmacokinetic parameters of both etoposide and etoposide catechol were calculated using the WinSAAM modeling program developed at NIH.**

Results: **The mean maximum concentration (C_{max}) for total (0.262 ± 0.107 μg/ml) and free catechol (0.0186 ± 0.0082 μg/ml) on day 5 were higher than the mean C_{max} for total (0.114 ± 0.028 μg/ml) and free catechol (0.0120 ± 0.0091 μg/ml) on day 1. The mean area under the plasma concentration-time curve ($AUC)_{24h}$ for total (105.4 ± 49.1 μg.min/ml) and free catechol (4.89 ± 2.23 μg.min/ml) on day 5 were much greater ($P < 0.05$) than those for total (55.9 ± 16.1 μg.min/ml) and free catechol (3.04 ± 1.04 μg.min/ml) on day 1. In contrast, the AUC_{24h} for etoposide was slightly lower on day 5 than on day 1.**

Conclusions: **The C_{max} and AUC_{24h} for etoposide catechol were significantly higher on day 5 than on day 1. This suggests that metabolism of etoposide to its catechol metabolite increases in pediatric patients receiving multiple-day bolus etoposide infusions. These findings may be relevant to future reduction of the risk of leukemia as a treatment complication, because etoposide and etoposide catechol are both genotoxins.**

INTRODUCTION

Etoposide (scheme 1) is a semisynthetic epipodophyllotoxin analog that has been used since the 1980s as a highly efficacious anticancer drug for the treatment of many different adult and pediatric solid tumors and leukemias (1). However, introduction of epipodophyllotoxins into clinical usage led to the recognition of a form of secondary leukemia characterized by balanced chromosomal translocations as a treatment complication (2–5). The overall incidence of leukemia after epipodophyllotoxin-containing regimens is approximately 2–3% (6), but the incidence has been higher with intermittent weekly or twice weekly scheduling (7) and with more intensive treatments (8). When the National Cancer Institute Cancer Therapy Evaluation Program monitored the occurrence of leukemia in 12 clinical trails using low (<1500 mg/m^2), moderate (1500–2999 mg/m^2), or high (>3000 mg/m^2) epipodophyllotoxin cumulative doses, the lack of a dose-response effect suggested that factors other than cumulative dose of the parent drug are the primary determinants of risk (6).

One of the major pathways of etoposide metabolism involves *O*-demethylation to etoposide catechol by cytochrome P450 3A4 (CYP 3A4; Fig. 1; Refs. 9, 10). The promoter region of the *CYP3A4* gene is polymorphic. We have reported previously that the wild-type *CYP3A4* genotype increases and the variant *CYP3A4* genotype decreases the risk of epipodophyllotoxin-related leukemias with translocation of the *MLL* gene at chromosome band 11q23 (11). Etoposide catechol can undergo sequential one-electron oxidation steps to etoposide semiquinone and etoposide quinone (12, 13). The quinone metabolite is a Michael acceptor, which could damage cells through alkylation of crucial cellular macromolecules including DNA and proteins (12–17). In addition, subsequent redox cycling initialized by etoposide catechol can result in the formation of reactive oxygen species (14). Reactive oxygen species can either damage DNA directly (18) or initiate lipid peroxidation. The resulting lipid hydroperoxides can then undergo homolytic decomposition to form DNA-reactive aldehydic bifunctional electrophiles, such as malondialdehyde, 4-hydroxy-2-nonenal, and 4-oxo-2-nonenal (19). Thus, etoposide metabolites as well as the parent drug are genotoxins.

Received 9/16/03; revised 12/31/03; accepted 2/5/04.

Grant support: NIH Grant CA77683, NIH General Clinical Research Center Grant MO1-RR00240, and the Pediatric Pharmacology Research Unit of the Children's Hospital of Philadelphia NIH Grant UO1 5-U01-HD-37255.

Note: N. Zheng is currently at the Department of Clinical Discovery Analytical Science, Bristol-Myers Squibb Co., 1 Squibb Drive, New Brunswick, NJ 08903. S. Pang is currently at the Pharmacokinetics and Drug Metabolism Department, Purdue Pharma, L.P., 444 Saw Mill River Road, Ardsley, NY 10502.

The costs of publication of this article were defrayed in part by the payment of page charges. This article must therefore be hereby marked *advertisement* in accordance with 18 U.S.C. Section 1734 solely to indicate this fact.

Requests for reprints: Carolyn Felix, Abramson Research Building, Room 902B, Division of Oncology, The Children's Hospital of Philadelphia, 3615 Civic Center Boulevard, Philadelphia, PA 19104-4318. Fax: (215) 590-3770; E-mail: felix@email.chop.edu.

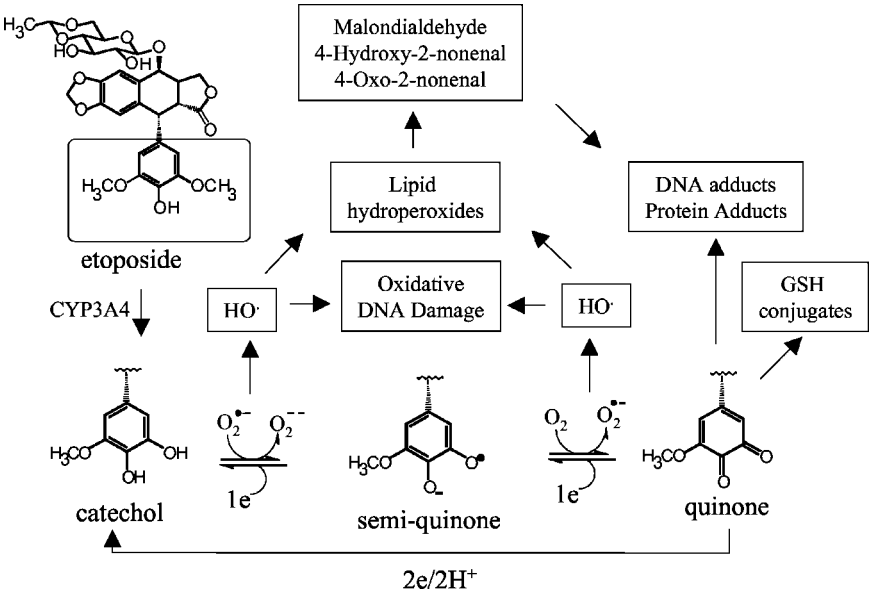

Fig. 1 Metabolism of etoposide: formation of etoposide catechol, etoposide semiquinone, and etoposide quinone.

The primary mechanism of cytotoxicity of etoposide and the basis for its antineoplastic action involves DNA topoisomerase II-mediated chromosomal breakage that initiates apoptosis (20–22). It has been suggested that the same mechanism of DNA damage may lead to translocations (5). However, the *O*-demethylated metabolites of etoposide have cytotoxic properties that are as potent as the parent drug (17). These etoposide metabolites like the parent drug increase the formation of DNA topoisomerase II cleavage complexes (23, 24), and can damage *MLL* and its partner genes by enhancing DNA topoisomerase II cleavage (25, 26).

The anticancer activity of etoposide has been demonstrated to be schedule-dependent (27). Despite several studies conducted in adults and children on the efficacy and safety of different schedules of etoposide, the optimal schedule has not been determined (28, 29). On the basis of the observation that five consecutive daily 2-h infusions of 100 mg/m^2 resulted in etoposide concentrations above 1 μg/ml for a significantly longer time (96.5 h) than a 500 mg/m^2 continuous infusion over 24-h (46 h), common schedules for etoposide treatment involve multiple-day dosing (30). However, multiple-day dosing could be harmful if plasma concentrations of etoposide and/or its genotoxic metabolites increase during the course of treatment.

We reported previously the simultaneous analysis of etoposide and its catechol metabolite as protein-free and total concentrations in plasma samples from pediatric patients using liquid chromatography/tandem mass spectrometry methodology (31). The purpose of the present study was to elaborate a pharmacokinetic model for etoposide and its catechol metabolite during a conventional multiple-day schedule that is often used in children. The model was developed to determine specific rate constants for individual compartments and to provide a mathematical description of individual pathways that are involved in etoposide disposition.

PATIENTS AND METHODS

Patients. The Institutional Review Board of the Children's Hospital of Philadelphia and the Institutional Review Board of the University of Pennsylvania approved this research. Seven patients (four girls and three boys) participated in the study including four patients with Ewing's sarcoma, two patients with Hodgkin's disease, and one patient with non-Hodgkin's lymphoma (Table 1). Ages were between 11 years 7 months and 16 years 2 months at time of diagnosis (14.0 ± 1.9; mean ± SD). Their heights were between 144 and 187.6 cm

Table 1 Patient characteristics

Patients	Diseases	Sex	Age (years. months)	Height (cm)	Weight (kg)	Area (M^2)	Target (mg/m^2)	Infusion time (h)
1	Ewing's sarcoma	F	11.7	144	44.3	1.30	100	1
2	Ewing's sarcoma	F	12.0	148	36.9	1.23	100	1
3	Hodgkin's disease	F	13.7	164	54.8	1.58	100	1
4	Ewing's sarcoma	M	13.6	159	50.9	1.50	100	1
5	Non-Hodgkin's lymphoma	M	14.6	172	70.8	1.84	100	1
6	Ewing's sarcoma	F	16.2	170	88.0	2.00	100	1
7	Hodgkin's disease	M	15.6	187.6	137.6	2.68	100	1
Mean ± SD			14 ± 1.9	164 ± 15.9	69 ± 34.7	1.73 ± 0.50		

(164 ± 15.9 cm; mean ± SD) and weights were between 36.9 and 137.6 kg (69 ± 34.7 kg; mean ± SD). All of the patients received etoposide at a dose of 100 mg/m^2 as a 1-h infusion daily for 5 days as part of an etoposide/ifosfamide-containing regimen. One patient received etoposide as the etoposide equivalent etopophos for 4 of the 5 days because of an allergic reaction (Table 1). Serial blood samples were obtained at predose and over 24 h after treatment on days 1 and 5.

Biological Sample Collection and Handling. Blood samples were taken from each patient at selected time points before and after completion of the infusion on days 1 and 5. In a typical study, the blood samples were taken at time 0 (immediately before etoposide infusion), and 0.5 h (midway in the etoposide infusion), 1 h (immediately at the end of infusion), 1.25 h, 1.5 h, 2 h, 3 h, 4 h, 6 h, 8 h, 10 h, 12 h, and 24 h after the etoposide infusion was begun. The blood samples were kept on ice and centrifuged at 3000 rpm for 10 min at 10°C. Plasma was stored immediately in a −80°C freezer. To obtain protein-free plasma, plasma (0.5 ml) was added to a Centrifree filter (Millipore) and centrifuged at 10°C for 60 min at 1900 × *g*. The protein-free plasma samples were also stored at −80°C.

Assay of Study Samples. Etoposide and etoposide catechol were extracted from the plasma or protein-free plasma and analyzed using liquid chromatography/tandem mass spectrometry as described previously (31). Teniposide, which is an analog of etoposide, was used as the internal standard. In summary, for the quantification of total etoposide and its catechol in plasma samples, 50 μl of plasma (standard samples, quality control samples, or patient samples), 20 μl teniposide solution (internal standard, 10 μg ml^{-1}), 20 μl freshly made ascorbic acid solution (50 mM), and 260 μl acetonitrile were added to an Eppendorf centrifuge tube. After vortex mixing for 5 min, the sample tubes were centrifuged in an Eppendorf 5415C centrifuge at 14,000 rpm for 5 min. The supernatant of each sample was transferred into another Eppendorf centrifuge tube and evaporated to dryness under a stream of nitrogen. The residues were reconstituted in 200 μl of 34% acetonitrile in water (initial mobile phase for high-performance liquid chromatography gradient). The sample solutions were filtered through a Costar spin-X filter (2 μm) and transferred to autosampler vials, and 20 μl of each solution was injected into the high-performance liquid chromatography system. The procedure for the protein-free fraction analysis was the same as for total plasma except that 200 μl of protein-free plasma was used instead of 50 μl of plasma, and the amount of acetonitrile was increased to 800 μl. Reversed-phase chromatography was performed on a YMC (Wilmington, NC) octadecyl silane analytical column (150 × 2.0 mm inside diameter; 3 μm) using a Waters (Milford, MA) Alliance 2690 high-performance liquid chromatography system. The mobile phase consisted of 5 mM ammonium formate and 0.1% aqueous formic acid solution with 10% acetonitrile as A and 90% acetonitrile as B at a flow rate of 0.2 ml/min. Mass spectra were acquired on a Finnigan TSQ7000 triple-quadrupole mass spectrometer (Thermo Finnigan, San Jose, CA) equipped with an electrospray ionization source. The mass spectrometer was operated in the positive ionization mode, and nitrogen was used as both sheath gas (70 psi) and auxiliary gas (25 units). The source was maintained at 200°C and the needle potential at 4.5 kV. The multiplier voltage was set at 1500 V, and argon was used as the collision gas at 3.5 mTorr (1 Torr = 133.3 Pa). The mass spectrometer was configured in the selected reaction monitoring mode with a transition of *m/z* 606 → *m/z* 229 for etoposide, *m/z* 592 → *m/z* 229 for etoposide catechol, and *m/z* 674 → *m/z* 383 for teniposide (internal standard). The collision energy offset was set at −32 eV for both etoposide and teniposide, and −25 eV for etoposide catechol. The linear ranges for the standard curves were 0.2–100 μg/ml for total etoposide analysis, 10–5,000 μg/ml for total catechol analysis, 25–15,000 ng/ml for free etoposide analysis, and 2.5–1,500 ng/ml for free catechol analysis. The data were analyzed by using LCQuan Ver 1.2. Quantification was achieved by plotting the peak area ratio of the analytes to the internal standard *versus* concentration followed by linear regression analysis with a weighting factor of $1/x^2$. The plasma or protein-free plasma quality controls for each analyte were prepared, stored, and assayed with the study samples. The standard curves were linear with $R^2 \geq 0.997$. The predicted concentrations of the quality control samples were between 94% and 108% of their nominal values. The intra-day and inter-day assay variability was <6.5%. The standard curve and quality control samples indicated that the assay method had good precision and accuracy, and that the analytes were stable under the storage and assay conditions.

Pharmacokinetic Analysis. All of the modeling was conducted using the WinSAAM kinetic modeling software developed at NIH (32).[5] A weighted least-squares approach was used to fit the total etoposide, total catechol, free etoposide, and free catechol simultaneously, leading to the direct estimates of the adjustable rate constants. For all of the data fitting, rate parameters were considered resolved when their fractional SDs were <0.3 (or 30%). No estimated parameters had a fractional SD >20%. Statistical analyses of pharmacokinetic parameters were conducted using STATA 7 software (STATA Corporation, College Station, TX). Using the (no constant) no Y intercept option in STATA 7, day 5 parameter values were regressed against the corresponding day 1 parameters. If the regression slope was significantly different from day 1, then the day 5 parameter value was deemed significantly different from the corresponding day 1 parameter.

RESULTS

A first order four-compartment model (Fig. 2) was used to fit the plasma concentration, and the protein-free plasma concentrations of etoposide and its catechol metabolite for each of the 7 patients. This model accounted for both elimination and metabolism. The distribution spaces of free etoposide and free etoposide catechol were assumed to be the same and constrained to be equal to the extracellular fluid volume, which is ~21% of bodyweight (Table 2; Ref. 33). This assumption provided the best fit to the data. The distribution spaces for protein-bound etoposide and etoposide catechol were also assumed to be the same, and were estimated to be 15.7 ± 1.1 and 13.5 ± 3.5% of bodyweight on days 1 and 5, respectively (Table 2). Thus, the distribution volume

[5] Internet address: http://www.WinSAAM.com.

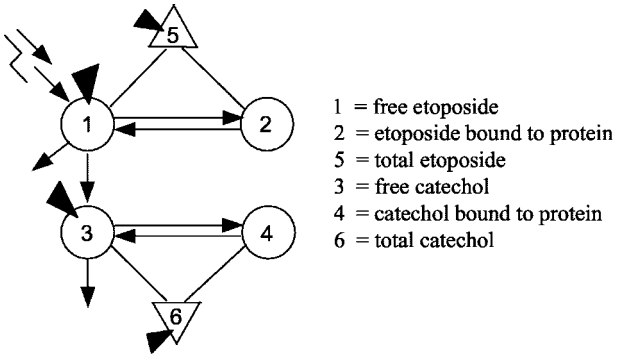

Fig. 2 Pharmacokinetic model for etoposide metabolism to its catechol metabolite. Etoposide was infused as free fraction to compartment 1. The ▼ represent the plasma samples taken for liquid chromatography/mass spectrometry analysis. *1,* free etoposide; *2,* etoposide bound to protein; *5,* total etoposide; *3,* free catechol; *4,* catechol bound to protein; *6,* total catechol.

Table 2 Pharmacokinetic parameters obtained from 7 patients (mean ± SD) from the model described in Fig. 1

Parameter	Day 1	Day 5
Body weight (kg)	69.1 ± 34.7	69.1 ± 34.7
Volume of distribution for free etoposide or catechol (ml)	14764 ± 6523	14550 ± 7056
Volume of distribution for protein bound etoposide or catechol (ml)	10537 ± 6067	9414 ± 5366
Volume of distribution for free etoposide or catechol (% of body weight)	21.8 ± 2.3	21.2 ± 1.1
Volume of distribution for protein bound etoposide or catechol (% of body weight)	15.7 ± 1.1	13.5 ± 3.5
K(0,1) (/min)	0.0615 ± 0.0283	0.0803 ± 0.0412[a]
K(2,1) (/min)	1.22 ± 1.49	1.19 ± 1.23
K(1,2) (/min)	0.0728 ± 0.0747	0.0877 ± 0.0849
K(3,1) (/min)	0.00234 ± 0.00188	0.00744 ± 0.00710
K(4,3) (/min)	1.22 ± 1.49	1.19 ± 1.23
K(3,4) (/min)	0.0728 ± 0.0747	0.0877 ± 0.0849
K(0,3) (/min)	0.153 ± 0.111	0.265 ± 0.290
Conversion of etoposide to catechol (%)	3.6 ± 3.0	14.4 ± 22.2

[a] Day 5 parameter was significantly different ($P < 0.05$) from corresponding day 1 parameter.

of protein-bound etoposide and etoposide catechol is approximately three times the plasma volume (33). Because plasma volume is ~5% of bodyweight, this indicates that approximately two-thirds of etoposide and its catechol are bound to proteins outside of the vascular space, perhaps to proteins on the vascular walls or to protein binding sites in well-vascularized tissue such as liver, spleen, and muscle.

The intercompartment rate constants for etoposide catechol were assumed to have the same values as the corresponding rate constants describing the movement of etoposide. A representative plasma concentration of total etoposide, total etoposide catechol, free etoposide, and free etoposide catechol concentration *versus* time curve is shown in Fig. 3. The pharmacokinetic parameters obtained from WinSAAM modeling for total and free etoposide and etoposide catechol are summarized in Tables 2–4. On the basis of the model shown in Fig. 2, the distribution half-lives ($t_{1/2\alpha}$) for free etoposide ranged from 10.0 to 56.9 min on day 1, and from 9.2 to 92.0 min on day 5. For free etoposide catechol, the distribution half-lives ($t_{1/2\alpha}$) ranged from 10.1 to 54.5 min on day 1 and from 22.1 to 52.4 min on day 5. The elimination half-lives ($t_{1/2\beta}$) for free etoposide ranged from 200 to 332 min on day 1 and from 86.3 to 481 min on day 5. For free etoposide catechol, the elimination half-lives ($t_{1/2\beta}$) ranged from 80.7 to 410 min on day 1 and from 74.4 to 332 min on day 5. As shown in Table 4, the mean maximum plasma concentration for total etoposide catechol (0.262 ± 0.107 μg/ml) on day 5 was higher ($P < 0.05$) than that for total etoposide catechol (0.114 ± 0.028 μg/ml) on day 1. Similarly, the mean free etoposide catechol concentration on day 5 (0.0186 ± 0.0082 μg/ml) was higher than on day 1 (0.0120 ± 0.0091 μg/ml).

The mean area under the plasma concentration-time curve $(AUC)_{24h}$ for total etoposide (3358 ± 968 μg·min/ml) and free etoposide (156 ± 55 μg·min/ml) on day 5 were significantly ($P < 0.05$) less than those for total etoposide (3966 ± 1268 μg·min/ml) and free etoposide (207 ± 54 μg·min/ml) on day 1 (Table 3). In contrast, the mean AUC_{24h} for total etoposide catechol (105.4 ± 49.1 μg·min/ml) and free etoposide catechol (4.89 ± 2.23 μg·min/ml) on day 5 were much greater than the mean AUC_{24h} for total etoposide catechol (55.9 ± 16.1 μg.min/ml) and free etoposide catechol (3.04 ± 1.04 μg·min/ml) on day 1 (Table 4). Similar results were observed for the AUC_{6h} (Ta-

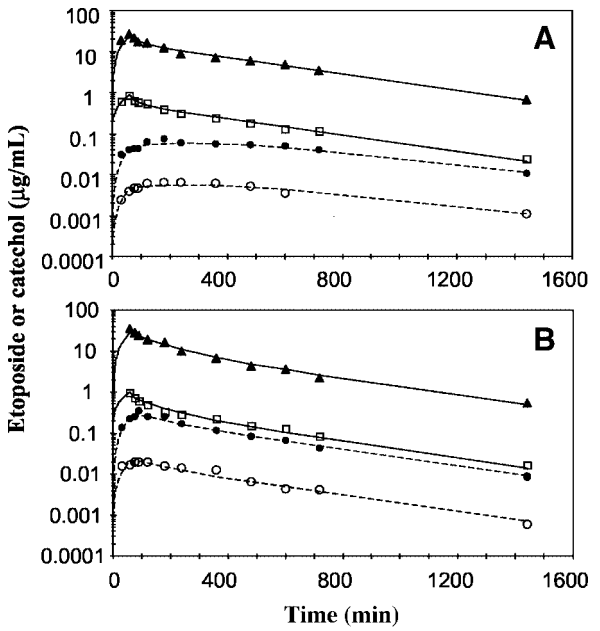

Fig. 3 Plasma concentration-time profiles for a subject given 100 mg/m^2 dose of etoposide for 1 h. Total etoposide (▲), total etoposide catechol (●), protein-free etoposide (□), protein-free etoposide catechol (○). Calculated values for etoposide ———; etoposide catechol ----. *A,* day 1. *B,* day 5.

Table 3 Pharmacokinetic parameters (mean ± SD) for total and protein-free etoposide from 7 patients

Parameter	Total etoposide on day 1	Total etoposide on day 5	Free etoposide on day 1	Free etoposide on day 5
C_{max}[a] (μg/ml)	24.1 ± 6.7	24.5 ± 5.6	1.28 ± 0.77	0.78 ± 0.14[b]
t_{max} (min)	60.1 ± 0.4	60.1 ± 0.4	60.7 ± 1.9	62.1 ± 5.7
$t_{1/2}\alpha$ (min)	65.3 ± 24.3	61.7 ± 14.9	30.7 ± 17.9	47.1 ± 33.9
$t_{1/2}\beta$ (min)	267 ± 67	271 ± 129	256 ± 51	220 ± 141
AUC_{6h} (μg·min/ml)	2788 ± 648	2586 ± 458	154 ± 36	123 ± 25[b]
AUC_{24h} (μg·min/ml)	3966 ± 1268	3358 ± 968[b]	207 ± 54	156 ± 55[b]
Mean residence time (min)	286 ± 78	240 ± 80	257 ± 78	213 ± 78

[a] C_{max}, maximum concentration; t_{max}, time of maximum concentration; $t_{1/2\alpha}$, distribution half-life; $t_{1/2\beta}$, elimination half-life; AUC, area under the plasma concentration-time curve.
[b] Day 5 parameter was significantly different ($P < 0.05$) from corresponding day 1 parameter.

bles 3 and 4). Other pharmacokinetic parameters on day 1 were generally similar to day 5 (Tables 2–4). However, the fractional rate constant K(0,1) for the elimination of etoposide (renal excretion and/or formation of other metabolites) was significantly greater ($P < 0.05$) on day 5 when compared with day 1 (Table 2).

DISCUSSION

Etoposide disposition in pediatric populations has been studied extensively and is similar to that in adults (34–36). However, there are only a few studies on the disposition of its major metabolite, etoposide catechol, in either adults or children (37–39). We have used a highly sensitive and specific liquid chromatography/tandem mass spectrometry assay for the simultaneous determination of both the total and free fraction of etoposide and its catechol metabolite in plasma in a pediatric population. Using WinSAAM modeling, we have demonstrated that both the free and total (free + noncovalently protein-bound) forms of the genotoxic catechol metabolite, but not etoposide, increased during multiple-day dosing in seven pediatric patients treated with etoposide for 5 days by conventional bolus i.v. dosing. In a prior study of adults receiving etoposide at myeloablative bolus 1-h doses of 600 mg/m^2/day for 4 days before hematopoietic stem cell transplantation for the therapy of germ cell tumors, the concentration of the catechol metabolite was also observed to increase from the first day to the last day of treatment (40). In a prior study of children receiving etoposide as a 2-h bolus dose of 300 mg/m^2, etoposide and etoposide catechol disposition were measured on a single day (39). The present study provides the first data on sequential, multiple-day etoposide catechol pharmacokinetics when etoposide was administered at conventional, nonmyeloablative doses in a pediatric population.

To begin elucidation of the mechanisms by which secondary leukemias occur after treatment with etoposide, it is important to fully understand the disposition of etoposide and its catechol metabolite in adults and children. In patients receiving etoposide for anticancer treatment, a substantial amount of plasma etoposide is noncovalently bound to plasma proteins with significant interpatient variation (41). The unbound (protein-free) fraction of etoposide correlates more closely with both toxicity and efficacy than the total drug concentration (42). Therefore, it is important to develop a rational pharmacokinetic model that is able to simultaneously determine the total and free fractions of etoposide and its catechol metabolite. On the basis of the WinSAAM modeling program, the best fit of the plasma and protein-free plasma concentration-time parameters was achieved by using a first-order four-compartment model shown in Fig. 2. With the same topology as that was described previously (31, 39), this model made it possible to simultaneously determine the pharmacokinetic parameters for total and free etoposide parent drug and its major catechol metabolite. The intercompartmental fractional transfer rates were not significantly different between day 1 and day 5. However, K(0,1), the fractional rate constant describing the elimination or removal of free etoposide, was significantly ($P < 0.05$) increased on day 5. We speculate that this might be a reflection of either an increase in excretion of etoposide or an increase in the rate of etoposide metabolism.

The mean maximum concentration for total etoposide catechol on day 5 (0.262 ± 0.107 μg/ml) was higher than on day 1 (0.114 ± 0.028 μg/ml; Table 4). The same trend was observed for free etoposide catechol (Table 4). These results suggest that exposure to the catechol metabolite increases in pediatric pa-

Table 4 Pharmacokinetic parameters (mean ± SD) for total and protein-free etoposide catechol from 7 patients

Parameter	Total catechol on day 1	Total catechol on day 5	Free catechol on day 1	Free catechol on day 5
C_{max}[a] (μg/ml)	0.114 ± 0.028	0.262 ± 0.107[b]	0.0120 ± 0.0091	0.0186 ± 0.0082
t_{max} (min)	150 ± 52	105 ± 39	137 ± 67	103 ± 29
$t_{1/2}\alpha$ (min)	41.4 ± 18.8	38.5 ± 13.5	30.7 ± 17.9	47.1 ± 33.9
$t_{1/2}\beta$ (min)	257 ± 115	194 ± 92	256 ± 51	220 ± 140[b]
AUC_{6h} (μg·min/ml)	28.7 ± 5.9	64.8 ± 29.3[b]	1.71 ± 0.66	3.18 ± 1.36[b]
AUC_{24h} (μg·min/ml)	55.9 ± 16.1	105.4 ± 49.1[b]	3.04 ± 1.04	4.89 ± 2.23[b]

[a] C_{max}, maximum concentration; t_{max}, time of maximum concentration; $t_{1/2\alpha}$, distribution half-life; $t_{1/2\beta}$, elimination half-life; AUC, area under the plasma concentration-time curve.
[b] Day 5 parameter was significantly different ($P < 0.05$) from corresponding day 1 parameter.

tients after multiple-day conventional bolus dosing. Among the patients studied, the inter-individual variability in maximum concentration was small and there were no obvious outliers. The mean AUC_{6h} and AUC_{24h} for total etoposide catechol on day 5 were greater than on day 1 (Table 4, Fig. 4). Similar results were observed for free etoposide catechol, the AUC_{6h} and AUC_{24h} for which also were significantly higher on day 5 than on day 1 (Table 4, Fig. 4). These results indicate that the patients were exposed to a higher concentration of etoposide catechol (total and free) on day 5 than on day 1. In contrast, the AUC_{24h} of total and free etoposide on day 5 were significantly less than on day 1 (Table 3, Fig. 5).

There are four possible mechanisms which could account for or contribute to the elevated concentrations and AUCs of total and free etoposide catechol observed on day 5:

1. Increased formation of etoposide catechol. On day 5, the fractional rate of formation of etoposide catechol K(3,1), 0.00744 ± 0.00710 was substantially although not statistically significantly greater than 0.00234 ± 0.00188 on day 1 (Table 2). In addition, the estimated % conversion of etoposide to etoposide catechol [K(3,1)/(K(0,1) + K(3,1)] was 14.4 ± 22.2 on day 5 compared with 3.6 ± 3.0 on day 1 (Table 2).

2. Decreased elimination of etoposide catechol. The mean fractional elimination rate of etoposide catechol on day 5 (0.265 ± 0.290), although not statistically significant ($P >$ 0.05), was numerically higher than that on day 1 (0.153 ± 0.111 min^{-1}), so this is unlikely to be the explanation.

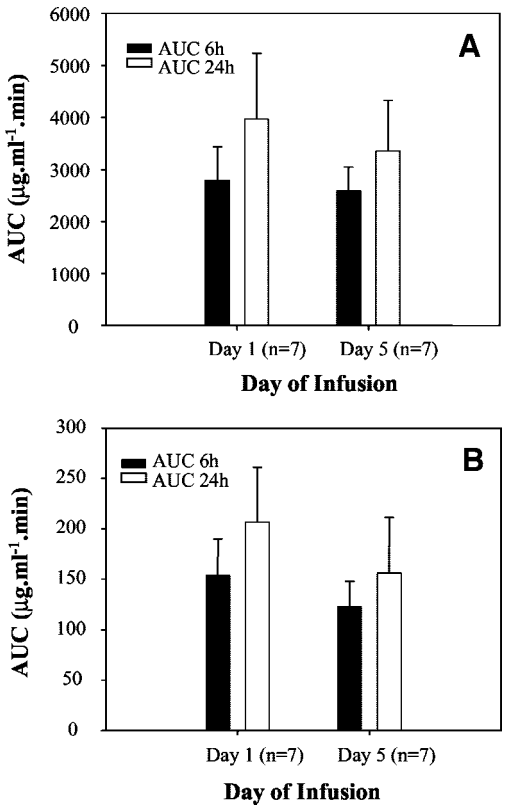

Fig. 4 Mean area under the curve of etoposide catechol in the plasma of 7 patients 6 h (■) or 24 h (□) after dosing with etoposide on day 1 compared with day 5. *A*, total etoposide catechol. *B*, free etoposide catechol; *bars*, ±SD.

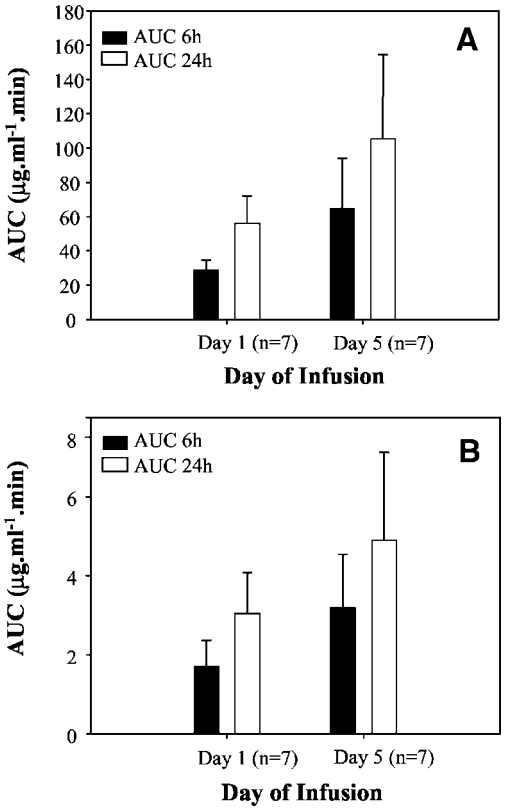

Fig. 5 Mean area under the curve of etoposide in the plasma of 7 patients 6 h (■) or 24 h (□) after dosing with etoposide on day 1 compared with day 5. *A*, total etoposide. *B*, free etoposide; *bars*, ±SD.

3. Decreased volume of distribution of etoposide catechol. From Table 2, the volume of distribution for free etoposide catechol is unchanged from day 1 to day 5 and, for protein-bound etoposide catechol, there is only a slight (nonsignificant) decrease in volume of distribution from 15.7 ± 1.1% of body weight on day 1 to 13.5 ± 3.5% of body weight on day 5. We speculate that this nonsignificant decrease in apparent volume of distribution of protein-bound etoposide and catechol may signify a slight increase in the concentration of catechol-binding proteins within plasma.

4. Accumulation of etoposide catechol from the dose of the previous day. The amount of etoposide catechol remaining in the body 24 h after a dose of etoposide depends upon the rate at which etoposide catechol is formed and the rate at which etoposide catechol is eliminated from the body. There is much individual variation in these two processes (Tables 2–6), and some subjects have relatively slow clearance of etoposide catechol. However, simulation analysis using kinetic parameters from day 1 indicates that accumulation of etoposide catechol in plasma due to the dosing of the previous day with etoposide accounts for a negligible amount of the increase in plasma catechol concentrations observed on day 5.

From our pharmacokinetic analysis, no single mechanism could be statistically identified as being a cause for the elevated

Table 5 Interpatient differences in AUC_{24h}[a] of etoposide

Patients	AUC (μg·min/ml) Total etoposide day 1	AUC (μg·min/ml) Total etoposide day 5	AUC ratio of day 5 to day 1	AUC (μg·min/ml) Free etoposide day 1	AUC (μg·min/ml) Free etoposide day 5	AUC ratio of day 5 to day 1
1	3901	3572	0.92	216	141	0.65
2	2874	2692	0.94	136	113	0.83
3	3644	2507	0.69	148	101	0.68
4	4515	4057	0.90	260	156	0.60
5	4759	3262	0.69	212	129	0.61
6	2109	2355	1.12	190	189	1.00
7	5958	5061	0.85	285	262	0.92
Mean ± SD	3966 ± 1268	3358 ± 968	0.87 ± 0.15	207 ± 54	156 ± 55[b]	0.76 ± 0.16[b]

[a] AUC, area under the plasma concentration-time curve.
[b] Day 5 parameter was significantly different ($P < 0.05$) from the corresponding day 1 parameter.

concentrations and AUCs of total and free etoposide catechol observed on day 5. However, our results are consistent with the possibility that a combination of increased rate of formation of etoposide catechol and decreased volume of distribution of etoposide catechol could together be responsible for the elevated concentrations and AUCs of total and free etoposide catechol observed on day 5.

Etoposide catechol is formed primarily through CYP3A4 metabolism (10). Our results are consistent with the possibility that during multiple-day dosing the enzyme is induced, resulting in increased etoposide metabolism, with concomitant increased formation of the catechol metabolite. In fact a recent study using a mouse model system has reported that etoposide can induce pregnane X receptor-mediated CYP3A4 transcription (43). However, little is known about the relative importance of CYP3A5 in the metabolism of etoposide and it is also conceivable that induction of this enzyme (44) could contribute to the increased formation of the catechol metabolite. Studies are currently in progress to distinguish these two possibilities. Another factor that may have influenced the pharmacokinetic profiles in this study was the concurrent administration of ifosfamide as part of the multiple-agent regimen. No changes in the maximum concentration, mean AUC_{6h}, or AUC_{24h} were observed for free or total etoposide. Ifosfamide is known to induce CYP3A4 in primary hepatocytes maintained in culture (45). Therefore, it is possible that concurrent ifosfamide administration may have been of relevance to the increase in these parameters for free and total etoposide catechol observed between days 1 and 5. To investigate this latter possibility it would be necessary to perform the study with etoposide alone. However, because etoposide generally is used in multiagent regimens in patients, human hepatocytes in culture could be used to determine whether etoposide alone is able to induce its own metabolism.

Current approaches including chemotherapy and hematopoietic stem cell transplantation offer little hope for patients diagnosed with leukemia secondary to epipodophyllotoxin treatment. These leukemias are clinically aggressive and reported long-term survival rates are only approximately 10–20% (46, 47). The absence of PCR-detectable leukemia-associated chromosomal translocations in the bone marrow before the start of chemotherapy and the association of DNA topoisomerase II inhibitors but not other cytotoxic chemotherapeutic agents with leukemias with characteristic balanced translocations have suggested that DNA topoisomerase II inhibitors cause the translocations, which are essential aberrations in this form of leukemia (48, 49). One of the patients in this study has already been affected with leukemia as a treatment complication. Whereas this study demonstrates that in the pediatric population conventional multiple-day bolus dosing of etoposide is associated with increased formation of the genotoxic catechol metabolite from the first day to the last day of treatment, the risk of leukemia (approximately 2–3%) associated with such regimens (6), nonetheless, is less than that observed in the past with once weekly or twice weekly dosing (7). Safe etoposide regimens without any risk of leukemia are yet to be achieved. Studies of genetic

Table 6 Interpatient differences in AUC_{24h}[a] of etoposide catechol

Patients	AUC (μg·min/ml) Total catechol day 1	AUC (μg·min/ml) Total catechol day 5	AUC ratio of day 5 to day 1	AUC (μg·min/ml) Free catechol day 1	AUC (μg·min/ml) Free catechol day 5	AUC ratio of day 5 to day 1
1	64.3	114.5	1.78	3.56	4.52	1.27
2	33.5	40.7	1.22	1.59	1.72	1.08
3	42.6	54.2	1.27	1.73	2.19	1.27
4	59.8	132.8	2.22	3.49	5.12	1.47
5	82.9	183.2	2.22	3.68	7.27	1.98
6	48.6	86.1	1.77	4.37	6.92	1.58
7	60.1	125.9	2.10	2.88	6.51	2.26
Mean ± SD	55.9 ± 16.1	105.4 ± 49.1[b]	1.80 ± 0.42[b]	3.04 ± 1.04	4.89 ± 2.23[b]	1.56 ± 0.42[b]

[a] AUC, area under the plasma concentration-time curve.
[b] Day 5 parameter was significantly different ($P < 0.05$) from corresponding day 1 parameter.

variations in etoposide-metabolizing enzymes and pharmacokinetic studies of the genotoxic metabolites (such as etoposide catechol) may offer hope to identify at-risk individuals and arrive at safer regimens. Etoposide is a highly efficacious and important anticancer agent. Reduction in the risk of leukemia associated with its usage may be possible when at-risk individuals are identified and safer dosing regimens are developed. The finding in the present study that the currently favored multiple-day dosing regimen of etoposide results in increased metabolism to the genotoxic catechol metabolite will stimulate the search for alternative strategies that limit catechol formation.

REFERENCES

1. Henwood JM, Brogden RN. Etoposide. A review of its pharmacodynamic and pharmacokinetic properties, and therapeutic potential in combination chemotherapy of cancer. Drugs 1990;39:438–90.

2. Ratain MJ, Kaminer LS, Bitran JD, et al. Acute nonlymphocytic leukemia following etoposide and cisplatin combination chemotherapy for advanced non-small-cell carcinoma of the lung. Blood 1987;70: 1412–7.

3. Smith MA, Rubenstein L, Cazenave L, et al. Report of the Clinical Therapy Evaluation Program monitoring plan for secondary acute myeloid leukemia following treatment with epipodophyllotoxins. J Natl Cancer Inst 1993;85:554–8.

4. Smith MA, Rubenstein L, Ungerleider RS. Therapy-related acute myeloid leukemia following treatment with epipodophyllotoxins: estimating the risks. Med Pediatr Oncol 1994;23:86–98.

5. Felix CA. Leukemias Related to Treatment with DNA Topoisomerase II Inhibitors. Med Pediatr Oncol 2001;36:525–35.

6. Smith MA, Rubenstein L, Anderson JR, et al. Secondary leukemia or myelodysplastic syndrome after treatment with epipodophyllotoxins. J Clin Oncol 1999;17:569–77.

7. Pui C-H, Ribeiro RC, Hancock ML, et al. Acute myeloid leukemia in children treated with epipodophyllotoxins for acute lymphoblastic leukemia. N Eng J Med 1991;325:1682–7.

8. Kushner BH, Heller G, Cheung N-KV, et al. High risk of leukemia after short-term dose-intensive chemotherapy in young patients with solid tumors. J Clin Oncol 1998;16:3016–20.

9. Relling MV, Evans R, Dass C, Desiderio DM, Nemec J. Human cytochrome P450 metabolism of teniposide and etoposide. J Pharmacol Exp Ther 1992;261:491–6.

10. Relling MV, Nemec J, Schuetz EG, Schuetz JD, Gonzalez FJ, Korzekwa KR. O-demethylation of epipodophyllotoxins is catalyzed by human cytochrome P450 3A4. Mol Pharmacol 1994;45:352–8.

11. Felix CA, Walker AH, Lange BJ, et al. Association of *CYP3A4* genotype with treatment-related leukemia. Proc Natl Acad Sci USA 1998;95:13176–81.

12. van Maanen JM, Lafleur MV, Mans DR, et al. Effects of the ortho-quinone and catechol of the antitumor drug VP-16–213 on the biological activity of single-stranded and double-stranded ϕX174 DNA. Biochem Pharmacol 1988;37:3579–89.

13. Mans DRA, Retel J, van Maanen JMS, et al. Role of the semiquinone free radical of the anti-tumour agent etoposide (VP-16–213) in the inactivation of single- and double-stranded ϕX174 DNA. Br J Cancer 1990;62:54–60.

14. Bolton JL, Trush MA, Penning TM, Dryhurst G, Monks TJ. Role of quinones in toxicology. Chem Res Toxicol 2000;13:135–60.

15. Haim N, Nemec J, Roman J, Sinha BK. In vitro metabolism of etoposide (VP-16–213) by liver microsomes and irreversible binding of reactive intermediates to microsomal proteins. Biochem Pharmacol 1987;36:527–36.

16. van Maanen JM, de Ruiter C, Kootstra PR, et al. Inactivation of ϕX174 DNA by the ortho-quinone derivative or its reduction product of the antitumor agent VP16–213. Eur J Cancer Clin Oncol 1985;21: 1215–8.

17. van Maanen JM, de Vries J, Pappie D, et al. Cytochrome P-450-mediated O-demethylation: A route in the metabolic activation of etoposide (VP-16–213). Cancer Res 1987;47:4658–62.

18. Demple B, Harrison L. Repair of oxidative damage to DNA: Enzymology and biology. Annu Rev Biochem 1994;63:915–48.

19. Blair IA. Lipid hydroperoxide-mediated DNA damage. Exp Gerontol 2001;36:1473–81.

20. Osheroff N. Effect of antineoplastic agents on the DNA cleavage/religation reaction of eukaryotic topoisomerase II: inhibition of DNA religation by etoposide. Biochemistry 1989;28:6157–60.

21. Osheroff N, Zechiedrich EL, Gale KC. Catalytic function of DNA topoisomerase II. BioEssays 1991;13:269–75.

22. Fortune JM, Osheroff N. Topoisomerase II as a target for anticancer drugs: when enzymes stop being nice. Prog Nucleic Acid Res and Molecular Biology 2000;64:221–53.

23. Gantchev TG, Hunting DJ. Inhibition of the topoisomerase II-DNA cleavable complex by the ortho- quinone derivative of the antitumor drug etoposide (VP-16). Biochem Biophys Res Commun 1997;237: 24–7.

24. Gantchev TG, Hunting DJ. The ortho-quinone metabolite of the anticancer drug etoposide (VP-16) is a potent inhibitor of the topoisomerase II/DNA cleavable complex. Mol Pharmacol 1998;53:422–8.

25. Lovett BD, Strumberg D, Blair IA, et al. Etoposide metabolites enhance DNA topoisomerase II cleavage near leukemia-associated *MLL* translocation breakpoints. Biochemistry 2001;40:1159–70.

26. Lovett BD, Lo Nigro L, Rappaport EF, et al. Near-precise interchromosomal recombination and functional DNA topoisomerase II cleavage sites at *MLL* and *AF-4* genomic breakpoints in treatment-related acute lymphoblastic leukemia with t(4;11) translocation. Proc Natl Acad Sci USA 2001;98:9802–7.

27. Slevin ML, Clark PI, Joel SP, et al. A randomized trial to evaluate the effect of schedule on the activity of etoposide in small-cell lung cancer. J Clin Oncol 1989;7:1333–40.

28. van der Gaast A, Vlastuin M, Kok TC, Splinter TA. What is the optimal dose and duration of treatment with etoposide? II. Comparative pharmacokinetic study of three schedules: 1 x 100 mg, 2 x 50 mg, and 4 x 25 mg of oral etoposide daily for 21 days Semin Oncol 1992;19: 8–12.

29. Funke I, Wiesneth M, Platow S, Kubanek B. Palliative cytoreduction in refractory acute leukemia: a retrospective study of 57 adult patients. Ann Hematol 2000;79:132–7.

30. van Maanen JM, Retel J, de Vries J, Pinedo HM. Mechanism of action of antitumor drug etoposide: a review. J Natl Cancer Inst 1988; 80:1526–33.

31. Pang S, Zheng N, Felix CA, Boston R, Blair IA. Simultaneous determination of etoposide and its catechol metabolite in the plasma of pediatric patients by liquid chromatography/tandem mass spectrometry. J Mass Spec 2001;36:771–81.

32. Greif P, Wastney M, Linares O, Boston R. Balancing needs, efficiency, and functionality in the provision of modeling software: a perspective of the NIH WinSAAM Project. Adv Exp Med Biol 1998; 445:3–20.

33. Guyton AC. Partition of body fluids: osmotic equilibria between extracellular and intracellular fluids. In: Textbook of Medical Physiology, Ed. 5. Philadelphia: WB Saunders Co., 1997. p. 424–437.

34. Lowis SP, Pearson AD, Newell DR, Cole M. Etoposide pharmacokinetics in children: the development and prospective validation of a dosing equation. Cancer Res 1993;53:4881–9.

35. Evans WE, Sinkule JA, Crom WR, Dow L, Look AT, Rivera G. Pharmacokinetics of Teniposide (VM26) and etoposide (VP16–213) in children with cancer. Cancer Chemother Pharmacol 1982;7:147–50.

36. Crom WR, Glynn-Barnhart AM, Rodman JH, et al. Pharmacokinetics of anticancer drugs in children. Clin Pharmacokinet 1987;12: 168–213.

37. van de Poll ME, Relling MV, Schuetz EG, Harrison PL, Hughes W, Flynn PM. The effect of atovaquone on etoposide pharmacokinetics in

children with acute lymphoblastic leukemia. Cancer Chemother Pharmacol 2001;47:467–72.

38. Relling MV, McLeod HL, Bowman LC, Santana VM. Etoposide pharmacokinetics and pharmacodynamics after acute and chronic exposure to cisplatin. Clin Pharmacol Ther 1994;56:503–11.

39. Relling MV, Yanishevski Y, Nemec J, et al. Etoposide and antimetabolite pharmacology in patients who develop secondary acute myeloid leukemia. Leukemia 1998;12:346–52.

40. Stremetzne S, Jaehde U, Kasper R, Beyer J, Siegert W, Schunack W. Considerable plasma levels of a cytotoxic etoposide metabolite in patients undergoing high-dose chemotherapy [letter]. Eur J Cancer 1997;33:978–9.

41. Liu B, Earl HM, Poole CJ, Dunn J, Kerr DJ. Etoposide protein binding in cancer patients. Cancer Chemother Pharmacol 1995;36: 506–12.

42. Stewart CF, Arbuck SG, Fleming RA, Evans WE. Relation of systemic exposure to unbound etoposide and hematologic toxicity. Clin Pharmacol Ther 1991;50:385–93.

43. Schuetz E, Lan L, Yasuda K, et al. Development of a real-time in vivo transcription assay: Application reveals pregnane X receptor-mediated induction of CYP3A4 by cancer chemotherapeutic agents. Mol Pharmacol 2002;62:439–45.

44. Kuehl P, Zhang J, Lin Y, et al. Sequence diversity in CYP3A promoters and characterization of the genetic basis of polymorphic CYP3A5 expression. Nat Genet 2001;27:383–391.

45. Chang TK, Yu L, Maurel P, Waxman DJ. Enhanced cyclophosphamide and ifosfamide activation in primary human hepatocyte cultures: response to cytochrome P-450 inducers and autoinduction by oxazaphosphorines. Cancer Res 1997;57:1946–54.

46. Sandler ES, Friedman DJ, Mustafa MM, Winick NJ, Bowman WP, Buchanan GR. Treatment of children with epipodophyllotoxin-induced secondary acute myeloid leukemia. Cancer 1997;79:1049–54.

47. Pui C-H, Relling MV, Rivera GK, et al. Epipodophyllotoxin-related acute myeloid leukemia: a study of 35 cases. Leukemia 1995;9:1990–6.

48. Megonigal MD, Cheung NK, Rappaport EF, et al. Detection of leukemia-associated MLL-GAS7 translocation early during chemotherapy with DNA topoisomerase II inhibitors. Proc Natl Acad Sci USA 2000;97:2814–9.

49. Blanco JG, Dervieux T, Edick MJ, et al. Molecular emergence of acute myeloid leukemia during treatment for acute lymphoblastic leukemia. Proc Natl Acad Sci USA 2001;98:10338–43.

Clinical Cancer Research

Plasma Etoposide Catechol Increases in Pediatric Patients Undergoing Multiple-Day Chemotherapy with Etoposide

Naiyu Zheng, Carolyn A. Felix, Shaokun Pang, et al.

Clin Cancer Res 2004;10:2977-2985.